Response of soil bacterial community composition and its associated geochemical parameters to rapid short-term cyclic groundwater-level oscillations: soil column experiments

Xuefeng Xia[a,c,d], Lirong Cheng[a,c,d], Yi Zhu[a,c,d], Yueqiao Liu[a,c,d], Kai Wang[a,c,d], Aizhong Ding[a,c,d,*], Zuansi Cai[b], Huansheng Shi[e], and Lili Zuo[e]

[a] College of Water Sciences, Beijing Normal University, Beijing 100875, China

[b] School of Engineering and the Built Environment, Edinburgh Napier University, Edinburgh EH10 5DT, UK

[c] Engineering Research Center of Groundwater Pollution Control and Remediation of Ministry of Education, Beijing Normal University, Beijing 100875, China

[d] Beijing Key Laboratory of Urban Hydrological Cycle and Sponge City Technology, Beijing Normal University, Beijing 100875, China

[e] China Railway Fifth Survey and Design Institute Group Co., Ltd., Beijing 102600, China

* Corresponding author. Present address: 12#, Xueyuannan Road, Haidian District, 100875 Beijing, China. *E-mail address*: ading@bnu.edu.cn (A. Ding).

Abbreviations: NF, natural fluctuations; NFC, natural fluctuation column; QS, quasi static; QSC, quasi static column; RDA, redundancy analysis; RI, rainfall infiltration; RIC, rainfall infiltration column; TOC, total organic carbon.

Core ideas

Water saturation and oxygen level oscillated with groundwater level during groundwater-level oscillations.

Soil bacterial community structure was dynamic at the class level due to water saturation, oxygen level and TOC removal.

Rainfall infiltration induced rapid short-term cyclic groundwater-level oscillations could significantly influence soil carbon cycle and bacterial community composition.

Photo

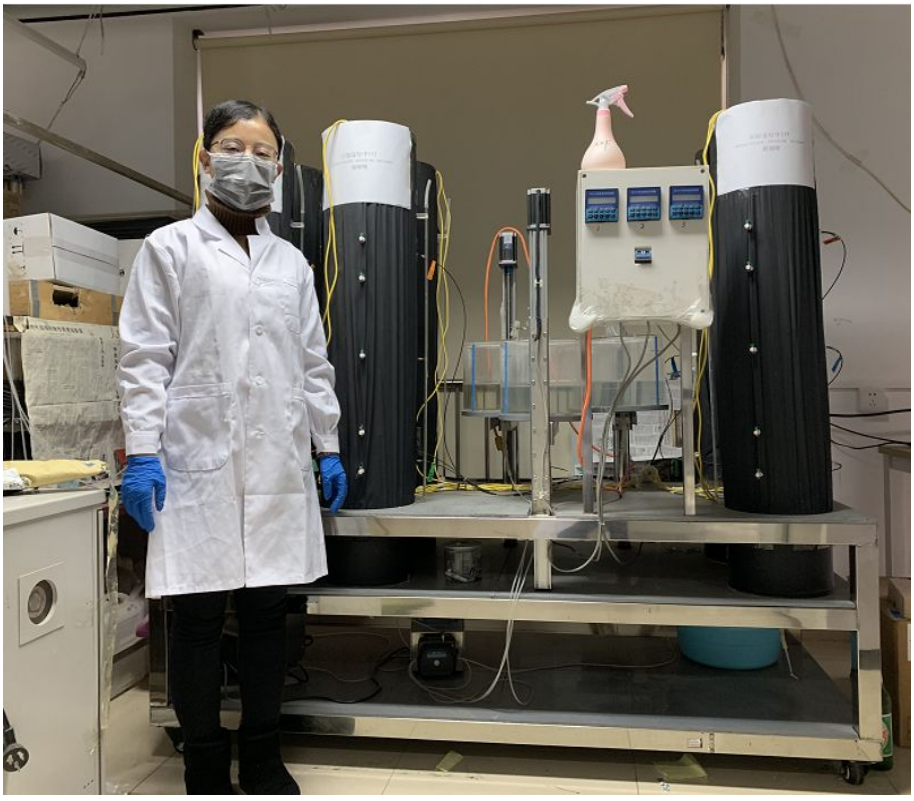

Abstract

Groundwater-level oscillations change geochemical conditions, carbon cycling processes and bacterial community composition, and these changes may vary vertically with depth in a soil. In this study, soil column experiments were conducted to explore variations in soil bacterial community composition and its associated geochemical parameters to rapid short-term cyclic groundwater-level oscillations driven by natural fluctuations (NF) and rainfall infiltration (RI) and the results are compared with quasi static (QS) column. Water saturation patterns in vadose and oscillated zones, and oxygen level patterns, soil total organic carbon (TOC) removal rates and soil bacterial community composition in vadose, oscillated and saturated zones were evaluated. Results showed that water saturation and oxygen level oscillated with groundwater level in NF and RI columns. TOC removal rates in RI column were the highest across vadose (~38.4%), oscillated (~35.8%) and saturated (~35.2%) zones. *Deltaproteobacteria*, which was significantly correlated with TOC removal ($p < 0.05$), exhibited relatively higher abundances in the vadose and oscillated zones of RI column than those of QS and NF columns. Soil bacterial community structure was dynamic at the class level due to water saturation, oxygen level and TOC removal. TOC removal was the driver to separate distribution of bacterial community structure in the vadose and oscillated zones of RI column from those of QS and NF columns. This study suggests that RI induced rapid short-term cyclic

52 groundwater-level oscillations could significantly influence both soil carbon cycle and
53 bacterial community structure in vadose and oscillated zones.
54

55 Introduction

56 Groundwater level usually oscillates due to hydrological dynamic factors such as natural
57 fluctuations (NF), groundwater-surface water interactions (Krause et al., 2007), rainfall
58 infiltration (RI) (Voisin et al., 2018), and anthropogenic factors like groundwater
59 extracting and recharging. Groundwater-level oscillations lead to transport and
60 redistribution of pollutants and soil components through interactions between soil and
61 water (Almasri 2007; Dai et al., 2019), and an alternating spatial-temporal distribution of
62 soil moisture and oxygen. These processes generate a depth profile in water saturation
63 and the availability of electron donors and terminal electron acceptors (Schimel et al.,
64 2007; Farnsworth and Hering, 2011; Zhou et al., 2015), which in turn cause soil bacterial
65 community to develop different functional diversity at different depths (Pett-Ridge and
66 Firestone, 2005). Soil bacterial communities can affect soil properties and quality through
67 numerous important biogeochemical processes (Lipson et al., 2012; Meckenstock et al.,
68 2015; Farnsworth et al., 2012), eventually resulting in an impact on ecosystem functions
69 (Huang et al., 2019). Therefore, it is important to investigate the response of soil bacterial
70 community composition at different depths to groundwater-level oscillations induced
71 geochemical conditions for better understanding the functions of soil ecosystems.

72

73 During groundwater-level oscillations, soil pore air may be replaced, or entrapped and
74 potentially dissolve into groundwater beneath groundwater level (Haberer et al., 2012;
75 Haberer et al., 2014; Machler et al., 2013; Jost et al., 2015), depending on the
76 hydrodynamics of specific imbibition pathway. Previous studies mostly focused on
77 groundwater-level oscillations driven by NF, which is characterized by an upward flow
78 of O_2-depleted groundwater that displaces soil pore air during increases in groundwater
79 level, and an influx of pore air drawn-in when groundwater level decrease, resulting in
80 alternating reducing and oxidizing conditions in oscillated zone (Yang et al., 2017). Less
81 attention has been paid to groundwater-level oscillations driven by RI. In contrast, RI is
82 charaterised by downward flow of oxygen-rich rainfall water that can entrap soil pore air
83 in vadose and oscillated zones, potentially elevating oxygen level in saturated zone (Van
84 Driezum et al., 2018; Neale et al., 2000). Hence, oxygen level along with soil moisture
85 content (or water saturation) will exhibit different temporal patterns within the vadose,
86 oscillated and saturated zones of an aquifer in response to NF and RI. As water and
87 oxygen are key factors that drive biogeochemical processes (Borer et al., 2018; Suenaga
88 et al., 2018), understanding the spatio-temporal distribution of water saturation and
89 oxygen level in an aquifer is therefore a necessary first-step to understanding the
90 response of bacterial community composition at various depths to groundwater level
91 variations. However, the effects of groundwater-level oscillations driven by these two

different hydrological dynamic factors (NF and RI) on the spatio-temporal distribution of water saturation and oxygen level have rarely been reported (Davis et al., 2013).

Some researchers have reported that groundwater-level oscillations can change spatial distribution and transformation of pollutants (Dobson et al., 2007; Yang et al., 2017) and cause bacterial community composition shifts (Zhou et al., 2015) in contaminated aquifers. However, the effect of groundwater-level oscillations on bacterial community composition in natural aquifers is still less known. As soils in natural aquifers are abundant in organic carbon (Vos et al., 2019), the leaching, dissolution and biodegradation of organic carbon can have an impact on response of soil bacterial community composition at different depths over long-term cyclic groundwater-level oscillations (Rühle et al., 2015). It is possible that an impact on response of soil bacterial community composition at different depths can also occur in natural aquifers over rapid short-term cyclic groundwater-level oscillations, as a previous study reported that short-term groundwater-level oscillations can alter geochemical processes (Farnsworth et al., 2012). Moreover, rapid short-term cyclic groundwater-level oscillations driven by NF and RI might cause different soil bacterial community composition responses. In order to understand the response of soil bacterial community composition at different depths to carbon cycle over rapid short-term cyclic groundwater-level oscillations driven by NF and RI, it is necessary to explore removal rates of soil TOC at different depths and their corresponding bacterial community compositions.

Therefore, the objectives of this study were to (1) delineate the spatio-temporal distribution of water saturation and oxygen level, (2) determine the removal rates of soil TOC, and (3) characterize the bacterial community composition at different depths in quasi static (QS) and two different rapidly oscillating aquifer scenarios (NF and RI). We tested the hypothesis that infiltration of oxygen-rich rainfall water into aquifers due to RI can alter soil total organic carbon (TOC) removal rates and bacterial community structure in a more pronounced way than during NF (both are compared with a QS). We discuss the link of soil TOC removal, water saturation and oxygen level related to bacterial community diversity and structure, and provide insight into the impacts of rapid short-term cyclic groundwater-level oscillations on the soil carbon cycle.

Materials and methods

Soil column and groundwater-level oscillation regime

To study the effects of rapid short-term cyclic groundwater-level oscillations on soil bacterial community and its associated geochemical parameters, three soil columns with a length of 120 cm and an internal diameter of 24 cm (Fig. 1) were established to represent the QS (control) and two different hydrological dynamic conditions (NF and RI). The soil columns were filled with natural fine-grained river sand collected from Cihe (Shijiazhuang, China), and basic physical and chemical properties of the soil are

summarized in Table S 1. The soils were packed into separate columns using a wet-packing procedure, i.e. the groundwater level was raised slowly to constantly maintain at a small depth of water above the top of soil surface to avoid entrapment of air but also to minimize the separation of grain sizes due to different settling rates. Groundwater was mimicked by O_2-depleted tap water (prepared by stripping the necessary amount of tap water with N_2), the physical and chemical properties of the groundwater are listed in Table S 2. The packed height was 110 cm, the compacted density was 1.60 g cm^{-3}, and the effective porosity was 0.35. The groundwater was fully drained after packing.

During the experiments, groundwater was injected from column bottom until the groundwater level reached a position 40 cm height (Table S 2, 6330 ml, which was calculated by soil porosity), and the groundwater level was maintained static for 12 hours. In the quasi static column (QSC), the groundwater level was maintained static throughout the experiments. In the natural fluctuation column (NFC) and rainfall infiltration column (RIC), three similar groundwater-level oscillation cycles were conducted using peristaltic pumps. Each cycle of groundwater-level oscillation includes: Firstly, the groundwater level was raised from 40 cm to 80 cm height by injecting groundwater from column bottom over a period of 10 hours at a flow rate 633 ml h^{-1} to simulate NF, while injecting rainfall water at the same flow rate from the top of column to simulate RI. The rainfall water was mimicked by tap water without any pretreatment, and the physical and

chemical properties of the rainfall water are listed in Table S 2. Secondly, the groundwater level in both NFC and RIC was maintained static at 80 cm height for 40 hours. Finally, the groundwater level in both NFC and RIC was dropped from 80 cm to 40 cm height by pumping groundwater out from column bottom at the flow rate 633 ml h^{-1} over a period of 10 hours. The groundwater level was maintained static at 40 cm height for 40 hours between cycles and for 12 hours after the last cycle. The estimated pattern of groundwater level based on the flow rate of peristaltic pumps within NFC and RIC during the experiments is also shown in Fig. 2 and Fig. 3. For the NFC and RIC, the cyclic oscillations of groundwater-level created a 40 cm thick oscillated zone between the vadose/unsaturated zone and saturated zone. Therefore, we define 80 - 110 cm height as a vadose zone (V), 40 - 80 cm height as an oscillated zone (O), and 0 - 40 cm height as a saturated zone (S) (Fig. 1).

Geochemical analysis

During the experiments, two TDR315L probes (Acclima, America) were placed in vadose and oscillated zone, respectively, to measure volumetric water content by a data collector CR300 (Campbell, America) (details can be found in the Supplementary Material). Water saturation was calculated by the ratio of measured volumetric water content with soil porosity. Three oxygen dipping probes (PreSens, Germany) were placed in vadose, oscillated and saturated zone, respectively. This is to measure the oxygen level by an OXY-10 trace SMA (PreSens, Germany) (details can be found in the

Supplementary Material).

Groundwater samples in the saturated zone were collected from QSC, NFC and RIC each at 0, 12, 22, 62, 72, 112, 122, 162, 172, 212, 222, 262, 272 and 284 h after the start of the experiments. All groundwater samples were collected in triplicate, filtered through a 0.45 μm Millipore filter to remove solid particles, and then stored at 4 ℃ until further analysis. The details regarding dissolved organic carbon (DOC) and UV-Visible measurement are described in the Supplementary Material.

At the end of the experiments, soil samples were collected from the vadose, oscillated and saturated zones of QSC, NFC and RIC each (more information can be found in the Supplementary Material). The soil samples collected from each zone were manually homogenized and divided into two parts. One part was dried naturally and passed through 100 mesh sieves. After removing inorganic carbon by acidification with 1% HCl, soil TOC was measured in triplicate using a Vario TOC system (Element, Germany) in the solid state at 950 °C. The other part was kept at -80 ℃ for the determination of soil bacterial community composition.

Soil bacterial community analysis

Total DNA was extracted from 0.250 g of soil using a PowerSoil DNA Kit (MOBIO, America) following the manufacturer's instructions (Wang et al., 2019). The V3-V4

194 hypervariable regions of bacterial 16S rRNA gene were amplified by polymerase chain
195 reaction (PCR) with primers 338F (ACTCCTACGGGAGGCAGCAG) and 806R
196 (GGACTACHVGGGTWTCTAAT) (Guo et al., 2018) (details can be found in the
197 Supplementary Material). To reduce PCR errors, amplification for each sample was
198 performed in triplicate and pooled together (Miao et al., 2017), and the amplicons were
199 extracted from 2% agarose gels and purified by using the AxyPrep DNA Gel Extraction
200 Kit (Axygen Biosciences, USA) following the manufacturer's instructions (Wang et al.,
201 2018), and quantified using QuantiFluor™-ST (Promega, USA) (Liu et al., 2018a). The
202 purified amplicons were sequenced on an Illumina MiSeq PE300 sequencer (Illumina,
203 USA) at Allwegene Technology Co., Ltd. (Beijing, China). Raw sequences were firstly
204 selected based on sequence length, quality, primer and tag (Yin et al., 2019) (details can
205 be found in the Supplementary Material). Alpha diversity analysis, including
206 Shannon-Wiener curve (Fig. S. 2), Good's coverage, Chao 1 and Shannon indices were
207 calculated by the Mothur package (version 1.34.4). Subsequently, singletons were
208 discarded to reduce the error rate with a small reduction in sensitivity (Zheng et al., 2019),
209 chimeric sequences were identified and removed using USEARCH (version 10). The
210 high-quality sequences were assigned operational taxonomic units (OTUs) with 97%
211 similarity (Liu et al., 2018a; Yin et al., 2019) using USEARCH (Version 10). The OTUs
212 were aligned with Silva128 16S rRNA database using the Ribosomal Database Project
213 (RDP) classifier (version 2.2) under the confidence threshold of 70% (Miao et al., 2017).
214 Different taxonomic groups were classified using quantitative insights into microbial

ecology (QIIME) package (version 1.2.1). The raw sequences have been deposited into the NCBI Sequence Read Archive under the accession number PRJNA573586.

Statistical analysis

Significant difference in the soil TOC removal rates among different columns was assessed by one-way analysis of variance (ANOVA) using SPSS 20. Based on detrended correspondence analysis (DCA) result (gradient length < 3.0), redundancy analysis (RDA) was selected to determine the multivariate correlations (Liu et al., 2018b) between bacterial community diversity, structure, water saturation, oxygen level and TOC removal using Canoco 4.5. Pearson correlation coefficients were also calculated and tested for significance using SPSS 20.

Results and Discussion

Spatio-temporal distribution of water saturation

For vadose zone, the water saturation in QSC increased at first few hours of the experiments, then gradually decreased over the experimental period (Fig. 2(a)). The increase of water saturation in first few hours is associated with the thickness of capillary rise. The slight decrease in water saturation over the experimental period is probably due to evaporation within vadose zone (Kong et al., 2015). For NFC and RIC, water saturation was synchronously oscillated with the rise and fall of groundwater level (Fig.

234 2(a)). However, the water saturation in RIC was higher than that of NFC, especially
235 during groundwater level recession period. This is mainly attributed to the differences in
236 the way the groundwater level was controlled. In RIC, the water harbored in vadose zone
237 was rainfall water that passed through vadose zone to oscillated zone. In contrast, the
238 water harbored in the vadose zone of NFC was groundwater that sucked by the capillary
239 forces which was limited by gravity and the height of groundwater level (Jost et al., 2015;
240 Hou et al., 2019).
241
242 For oscillated zone, the water saturation in NFC and RIC remained nearly stable from
243 start to 62 h and 162 h, respectively, and then periodically oscillated with the rise and fall
244 of groundwater level (between 50.89 - 98.69 %, and 39.49 - 100.00 %, respectively) (Fig.
245 2(b)). Compared to the cyclic oscillations of water saturation in NFC, the cyclic
246 oscillations of water saturation in RIC was delayed for one cycle. However, substantial
247 difference between NFC and RIC in each phase of the cyclic groundwater-level
248 oscillations was practically nonexistent after the groundwater table increased to the
249 highest level for the second time. This demonstrates that there is a time lag between RI
250 and the rise in groundwater level during the early stage of rapid short-term cyclic
251 groundwater-level oscillations driven by RI (Batayneh and Qassas 2006). The water
252 saturation in QSC gradually decreased from 94.63 % to 70.20 % (Fig. 2(b)), indicating
253 that groundwater in the oscillated zone of QSC was sucked by the upper drier soil (Baram

et al., 2012) and lost by evaporation related to temperature and air flow (Chen et al., 2019) under hydrostatic groundwater level conditions.

Spatio-temporal distribution of oxygen level

For vadose zone, the change patterns of oxygen level are similar in all three columns (Fig 3(a)). The oxygen level in QSC remained constant in first 70 hours of the experiments, and then slightly increased to the end of the experiments. This is probably because of a temporal increase of diffusive oxygen flux from air to the soil pores when water saturation exhibited the opposite trend (Neale et al., 2000). Notice that although the temporal distribution of oxygen level displayed similar trends for NFC and RIC associated with different imbibition and drainage cycles, overall, oxygen level was lower in NFC than that in RIC. This is because the infiltration of oxygen-rich rainfall water resulted in additional supply of oxygen to the vadose zone of RIC (Kohfahl et al., 2009), while the suction of oxygen-depleted groundwater (Haberer et al., 2015) led to the replacement of soil pore air and restricted the transport of air into the vadose zone of NFC (Dutta et al., 2015).

For oscillated zone, the oxygen level in NFC and RIC oscillated accordingly with the rise and fall of groundwater level (Fig 3(b)). This oscillation was within 4.20 - 7.25 mg L^{-1} in NFC, and within 4.40 - 7.45 mg L^{-1} in RIC. However, the oxygen level in QSC decreased from 6.41 mg L^{-1} to 5.28 mg L^{-1} at 115 h, and then increased to 7.40 mg L^{-1}. The oxygen

level of NFC oscillated over time with groundwater-level oscillations, decreased as groundwater level rose and increased as groundwater level dropped because the oscillated zone became a saturated zone with the rise of groundwater level. This could be explained by effective air contents, which were calculated by subtracting water saturation at a given location from the maximum effective porosity (McLeod et al., 2015). Notably, the oscillations of oxygen level in RIC were one cycle later than that in NFC, due to the higher water saturation in RIC being able to provide significant resistance to oxygen transport and groundwater re-oxygenation (Neale et al., 2000). The oxygen level in QSC decreased to the minimal value (115 h) and then gradually increased to the end of the experiments (Fig 3(b)) due to the effects of groundwater evaporation and re-oxygenation.

For saturated zone, the oxygen level in QSC continuously decreased from 2.47 mg L^{-1} to 0.52 mg L^{-1}, while in NFC it showed a continuous decline until ~ 80 h but an increase afterwards with a periodical oscillation between 1.38 mg L^{-1} and 2.71 mg L^{-1} (Fig 3(c)). For RIC, a long continuous decline of oxygen level was observed to be 0.15 mg L^{-1} at 247 h with a sharp increase to 2.63 mg L^{-1} in the end of the experiments. The continuous decrease of oxygen level in QSC indicates that the consumption of oxygen by organic carbon biodegradation or by other oxygen sinks in the soil was higher than the mass fluxes of oxygen replenished by advection and diffusion (Dutta et al., 2015). The periodical oscillations of oxygen level after ~ 80 h in NFC with returning to the similar level as the start of experiment probably due to the fact that oxygen was consumed by

redox reactions, re-oxygenation could also occur due to oscillations in groundwater level (Davis et al., 2013), which could lead to diffusion and entrapment of air or soil air in the groundwater below groundwater level (Neale et al., 2000). Effective oxygen entrapment could likely contribute to the rebound of oxygen in saturated zone since mass transfer of oxygen has been reported in an oscillating capillary fringe even under a single drainage or imbibition event (Haberer et al., 2012). The oscillation of oxygen level in RIC, however, was two cycles later than that in NFC, which demonstrated that oxygen input to saturated zone by RI was of minor importance and even less than oxygen consumption by redox reactions in saturated zone. This is because aerobic mineralization of organic carbon contained in the vadose and oscillated zones of RIC substantially consumed oxygen in rainfall water and air or soil air across the first two cycles (Datry et al., 2004). Interestingly, the last cycle showed a huge increase in the oxygen level, which might be due to the bacterial respiration-induced oxygen consumption decreasing as a result of labile organic carbon reduction after two cycles of groundwater-level oscillations, and more oxygen would be transported into the saturated zone. Although NF and RI appeared to have dissimilar effects on temporal distribution of oxygen level in saturated zone, cyclic NF and RI were all significant hydrological dynamic events with respect to providing oxygen to saturated zone compared with QS.

Variation in TOC removal with depth

The removal rates of soil TOC ranged from 1.60 ± 0.02 % to 38.36 ± 0.04 % across

315 vadose zones ($p < 0.05$), from 11.42 ± 0.03 % to 35.84 ± 0.01 % across oscillated zones
316 ($p < 0.05$) and from 26.71 ± 0.04 % to 35.16 ± 0.04 % across saturated zones ($p < 0.05$)
317 (Fig. 4). Among them, the vadose zone (38.36 ± 0.04 %) and oscillated zone (35.84 ±
318 0.01 %) of RIC achieved the highest TOC removal rates, followed by the saturated zones
319 of QSC, NFC and RIC. However, the removal rates of TOC in the vadose zone (1.60 ±
320 0.02 %) and oscillated zone (11.42 ± 0.03 %) of QSC were the lowest. This is because RI
321 caused a considerable amount of rainfall water to flow through the vadose and oscillated
322 zones, led to enhanced leaching, hydrolysis, biodegradation and dissolution of soil
323 organic carbon into soil solution (Gillefalk et al., 2018) that transported into the saturated
324 zone with groundwater level dropping (Chow et al., 2003).
325
326 The DOC concentrations in NFC and RIC exhibited cyclical responses, whereas the DOC
327 concentration in QSC increased from 3.43 mg L^{-1} to 4.96 mg L^{-1} (112 h), and then
328 decreased to 3.68 mg L^{-1} at the end of the experiments (Fig. S. 1(a)). It is worth noting
329 that the DOC concentration of most groundwater sampled at specific time in RIC was
330 lower than that in NFC. This demonstrates that DOC is likely to be mineralized by
331 bacterial communities in the vadose and oscillated zones of RIC under aerobic conditions
332 (Niu et al., 2017). The $SUVA_{254}$ and E_{253}/E_{203} in NFC and RIC alternated between high
333 and low values during rapid short-term cyclic groundwater-level oscillations, with a
334 downward trend in QSC (Fig. S. 1(b)). More importantly, UV absorbance at wavelengths
335 of 200-300 nm exhibited higher values in RIC and NFC than QSC at the end of the

experiments (Fig. S. 1(c)). Accordingly, we speculate that soil organic carbon acts as a great source of DOC and only high molecular compounds that can't be consumed by aerobic bacteria were left (Liu et al., 2019). Together with QSC, it is easy to judge from this study that enhanced carbon cycle (such as leaching, dissolution and biodegradation of soil organic carbon, releasing and aerobic mineralization of DOC) occurred as a result of rapid short-term cyclic groundwater-level oscillations and were especially driven by RI.

Variation in soil bacterial community composition with depth

Bacterial community diversity

For each sample, between 17,595 - 43,121 reads passed quality control (Table S 3). The coverage indices suggested that this was sufficient to give good coverage of the species present (Table 1 and Fig. S. 2). In vadose zone, the diversity indices (Chao 1 and Shannon) for RIC (RIC_V) were slightly lower than those for NFC (NFC_V) and QSC (QSC_V) (Table 1), in oscillated zone the diversity indices were very similar (RIC_O, NFC_O and QSC_O), whereas in saturated zone the bacterial community diversity of RIC (RIC_S) was higher than those of NFC (NFC_S) and QSC (QSC_S) (Table 1). The Venn diagrams illustrated that only 619 OTUs or 22% of the total OTUs were shared between QSC_S, NFC_S and RIC_S (Fig. S. 3), suggesting a relatively high level of dissimilarity in bacterial communities. The number of OTUs unique to RIC_S (713) was much higher than those in QSC_S and NFC_S (309 and 292). Other researchers have

356 demonstrated that soil bacterial community diversity can gradually decrease with
357 significant removal of soil organic carbon by leaching, dissolution and aerobic
358 transformation (Ning et al., 2018). This could explain the diversity differences between
359 the vadose zone communities, but not the similar diversity of the oscillated zone
360 communities or that the highest diversity in saturated zone was exhibited by RIC. Thus,
361 our results suggest other factors are also affecting diversity. For example, the downward
362 infiltration of oxygenated rainfall water in RIC probably transports more nutrients to the
363 saturated zone than in NFC or QSC, and this stimulate increased species diversity (Van
364 Driezum et al., 2018).

365 Bacterial community structure

366 To obtain detailed insights into bacterial communities, the phylogenetic classification of
367 bacterial sequences from the vadose, oscillated and saturated zones of three columns at
368 two taxonomic levels (phylum and class) is summarized in Fig. 5. The relative
369 abundances of top 10 phyla are shown in Fig. 5 (a), the composition of main bacterial
370 communities was similar, and the most abundant bacteria belonged to the phylum
371 *Proteobacteria* in all the samples (27.4 - 48.8%). Thus, it is concluded that the phylum
372 *Proteobacteria* is highly adapted to a wide range of water saturation. This finding is
373 consistent with previous reports indicating that *Proteobacteria* play a dominant role in
374 aquifers (Unno et al., 2015). The phylum *Acidobacteria* was observed as a second
375 abundant bacteria in vadose and oscillated zones. Similarly, *Gemmatimonadetes* and
376 *Actinobacteria*, which had been reported to be usually present in upper soil with relative

lower moisture (Huang et al., 2019; Zhou et al., 2019), were also more likely to be enriched in vadose and oscillated zones. The phyla *Firmicutes* and *Bacteroidetes* exhibited relatively higher abundances in the saturated zones of all three columns. Additionally, *Firmicutes* exhibited relatively higher abundances in RIC (16.6%) and NFC (11.4%) than QSC (8.8%), while *Bacteroidetes* exhibited relatively higher abundance in QSC (11.9%) than NFC (11.2%) and RIC (6.0%). A similar pattern to *Bacteroidetes* emerged when other bacterial communities, such as *Parcubacteria* or *Verrucomicrobia*, were considered.

The heat map of top 20 abundant classes of soil samples is presented in Fig. 5(b). The dominant classes in the same zone of different columns were similar, but the distribution of bacterial community structure differed in the three zones. The dominant classes in vadose zone were *Alphaproteobacteria*, *Betaproteobacteria* and *Gammaproteobacteria*. The most abundant class in QSC, NFC and RIC was *Betaproteobacteria* (11.6%), *Betaproteobacteria* (12.7%) and *Gammaproteobacteria* (14.8%), respectively. The dominant classes in oscillated zone were *Alphaproteobacteria* and *Betaproteobacteria*. The relative abundance of *Betaproteobacteria* in QSC (10.5%) was lower than those in NFC (12.2%) and RIC (12.2%). The dominant class in saturated zone was *Betaproteobacteria*, which exhibited similar relative abundances in all three columns (11.0 - 12.6%). This finding further revealed that *Betaproteobacteria* was appeared to be widely adapted to natural subsurface environments (Amano et al., 2012) and are highly

398 resistant to rapid short-term cyclic groundwater-level oscillations. The other dominant
399 classes included *Gemmatimonadetes*, *Sub_group6*, *Deltaproteobacteria*,
400 *Sphingobacteriia*, *Bacilli*, and *Clostridia* across the vadose, oscillated and saturated zones
401 of three columns. Among them, the relative abundance of *Deltaproteobacteria* was
402 higher in the oscillated and saturated zones of all three columns and the vadose zone of
403 RIC. The dominance of *Deltaproteobacteria* is attributed to their special heterotrophic
404 metabolic capabilities (Liu et al., 2019). That's the reason why *Deltaproteobacteria* was
405 usually found in low TOC residual soils and likely contribute to soil TOC removal (Table
406 2).
407
408 It is worth mentioning that the classes *Clostridia* and *Bacilli* in the same phylum
409 *Firmicutes* exhibited relatively higher abundances in the saturated zone of RIC (10.4%
410 and 6.5%) than those of NFC (7.0% and 4.2%) and QSC (4.1% and 5.0%). Conversely,
411 the *Sphingobacteriia* in the phylum *Bacteroidetes* exhibited relatively higher abundance
412 in QSC (7.6%) and NFC (4.7%). This might be because *Firmicutes* is one representative
413 of heterotrophic bacteria related to labile organic carbon removal (Scheff et al., 1984),
414 while *Bacteroidetes* is more likely to mineralize recalcitrant organic carbon (Li et al.,
415 2013). During the course of RI, more and more labile organic carbon is leached and
416 transported to the saturated zone, the bacterial communities that are able to biodegrade
417 labile organic carbon still occupied a relatively higher proportion. In contrary, the

418 biodegradable organic carbon presented in the saturated zone of QSC and NFC tends to
419 be refractory, which should be biodegraded by other functional bacterial communities.

420 Correlation between water saturation, oxygen level, TOC
421 removal and bacterial community composition

422 RDA analysis was performed to assess how hydrological conditions induced geochemical
423 conditions influence bacterial community diversity and bacterial community structure
424 (Fig. 6). Chao 1 and Shannon were chosen as diversity indices, and top 10 abundant
425 classes were selected to analyze distribution of bacterial community structure in RDA
426 ranking map. In RDA ranking map, distribution of sample (bacterial community structure)
427 is determined by correlations between top 10 abundant classes and geochemical
428 parameters. There is a negative correlation between TOC removal and Chao 1 and
429 Shannon indices. Distribution of bacterial community structure in RIC_V, RIC_O and the
430 saturated zones of all three columns had a negative correlation with Chao 1 and Shannon
431 indices as a result of higher TOC removal. This suggests the dominance of bacteria
432 capable of decomposing organic carbon in specific ways which might replace the
433 ecological niche of other bacterial communities (Zheng et al., 2019).
434
435 For classes, *Gammaproteobacteria* ($p < 0.05$), *Alphaproteobacteria* ($p < 0.05$),
436 *Actinobacteria* ($p < 0.05$) and *Gemmatimonadetes* had positive correlation with oxygen
437 level, *Betaproteobacteria*, *Deltaproteobacteria* ($p < 0.05$), *Clostridia*, *Cytophagia. Bacilli*,

438 and *Sphingobacteriia* had positive correlation with TOC removal, and
439 *Betaproteobacteria*, *Deltaproteobacteria*, *Clostridia*, *Cytophagia* ($p < 0.05$), *Bacilli* and
440 *Sphingobacteriia* ($p < 0.01$) had positive correlation with water saturation. For samples,
441 distribution of bacterial community structure varied in response to changes in water
442 saturation, oxygen level and TOC removal across the vadose, oscillated and saturated
443 zones of three columns. Distribution of bacterial community structure in the vadose and
444 oscillated zones of three columns was positively related to oxygen level. Distribution of
445 bacterial community structure in the saturated zones of all three columns was positively
446 related to water saturation. Distribution of bacterial community structure in the vadose
447 and oscillated zones of RIC was positively related to TOC removal, while distribution of
448 bacterial community structure in the vadose and oscillated zones of QSC and NFC was
449 negatively related to TOC removal. Therefore, TOC removal is the driver of
450 discriminating distribution of bacterial community structure in the vadose and oscillated
451 zones of RIC from those of NFC and QSC. This demonstrates that TOC removal can be
452 attributed to not only leaching and dissolution, but also biodegradation by bacterial
453 communities (Kolehmainen et al., 2007). Moreover, distinct differences in TOC removal
454 rates of the vadose and oscillated zones between NFC and RIC are related to the
455 imbibition pathways, which affect the leaching and dissolution of organic carbon.
456 Leaching and dissolution of organic carbon is a prerequisite for enhanced organic carbon
457 biodegradation under dry-wet alternation condition during rapid short-term cyclic
458 groundwater-level oscillations (Fig. S. 4). Overall, it can be concluded that rapid

459 short-term cyclic groundwater-level oscillations driven by RI can significantly affect
460 bacterial communities responsible for TOC removal in vadose and oscillated zones, while
461 rapid short-term cyclic groundwater-level oscillations driven by NF exhibit relatively
462 lower TOC removal rate and limit the responses of bacterial community structure.
463
464 Although bacterial community structure in the saturated zones of three columns were
465 obviously different (Fig. 5(b) and Fig. S. 3), oxygen level, TOC removal and water
466 saturation were not regulatory factors on the differences of bacterial community structure
467 distribution. Other biogeochemical processes might occur through a series of
468 transformation pathways (Lipson et al., 2012), which might account for the stimulation of
469 diverse dominant bacterial communities under similar TOC removal rates in the saturated
470 zones. Our results hint at a crucial role of RI in causing bacterial community structural
471 responses and carbon cycle within vadose and oscillated zones during rapid short-term
472 cyclic groundwater-level oscillations.
473

474 Conclusions

475 In this study, the effects of rapid short-term cyclic groundwater-level oscillations on the
476 spatio-temporal distribution of water saturation and oxygen level, removal rates of soil
477 TOC and soil bacterial community composition at different depths were analyzed. Water
478 saturation and oxygen level exhibited similar patterns in NFC and RIC. Across vadose,

oscillated and saturated zones, the TOC removal rates of RIC were higher than those of NFC and QSC. For vadose and oscillated zones, bacterial community structures in RIC differed from those of QSC and NFC. Meanwhile, oxygen level was the dominant contributor for reshaping bacterial community structures in the vadose and oscillated zones of all three columns. However, water saturation had a positive correlation with distribution of bacterial community structure in the saturated zones of all three columns. TOC removal positively correlated with distribution of bacterial community structure in the vadose, oscillated and saturated zones of RIC, as well as the saturated zones of NFC and QSC. Considering the patterns of TOC removal in the vadose, oscillated and saturated zones of RIC, we speculate that rapid short-term cyclic groundwater-level oscillations driven by RI could cause more possibility for leaching, dissolution and biodegradation of soil organic carbon. These results suggest the importance of considering hydrological dynamic factors in the prediction of the impacts of rapid short-term cyclic groundwater-level oscillations on soil bacterial community composition. Future studies should focus on the verification of the mechanisms linking functional bacterial communities to geochemistry by alternative means of detection.

Acknowledgments

This research was supported by the National Natural Science Foundation of China (No. 41672227) and National Key Research and Development Program of China (No. 12400211800015).

We are grateful to Prof. Douglas Ian Stewart (School of Civil Engineering, University of Leeds) for the English correction. We also greatly appreciate to the associate editor, Dr. Jinyun Tang, as well as anonymous reviewers for their helpful and constructive comments that contributed to improving the manuscript.

References

Almasri, M.N. 2007. Nitrate contamination of groundwater: A conceptual management framework. Environ. Impact Assess. Rev. 27:220-242.

Amano, Y., E. Sasao, T. Niizato, and T. Iwatsuki. 2012. Redox buffer capacity in water–rock–microbe interaction systems in subsurface environments. Geomicrobiol J. 29:628-639.

Baram, S., D. Kurtzman, and O. Dahan. 2012 Water percolation through a clayey vadose zone. J. Hydrol. (424-425):165-171.

Batayneh, A.T., and H.A. Qassas. 2006. Changes in quality of groundwater with seasonal fluctuations: an example from Ghor Sari area, southern Dead Sea coastal aquifers, Jordan. J. Environ. Sci. 18(2):263-269.

Borer, B., R. Tecon, and D. Or. 2018. Spatial organization of bacterial populations in response to oxygen and carbon counter-gradients in pore networks. Nat. Commun. 9:769.

Chen, C.F., J.E. Wu, X.A. Zhu, X.J. Jiang, W.J. Liu, H.H. Zeng, and F.R. Meng. 2019. Hydrological characteristics and functions of termite mounds in areas with clear dry and rainy seasons. Agric. Ecosyst. Environ. 277:25-35.

Chow, A.T., K.K. Tanji, and S. Gao. 2003. Production of dissolved organic carbon (DOC) and trihalomethane (THM) precursor from peat soils. Water Res. 37, 4475-4485.

Dai, L.C., X.W. Guo, F.W. Zhang, Y.G. Du, X. Ke, Y.K. Li, G.M. Cao, Q. Li, L. Lin, K. Shu, and C.J. Peng. 2019. Seasonal dynamics and controls of deep soil water infiltration in the seasonally-frozen region of the Qinghai-Tibet plateau. J. Hydrol. 571:740-748.

Datry, T., F. Malard, and J. Gibert. 2004. Dynamics of solutes and dissolved oxygen in shallow urban groundwater below a stormwater infiltration basin. Sci. Total Environ. 329:215-229.

Davis, G.B., D. Laslett, B.M. Patterson, and C.D. Johnston. 2013. Integrating spatial and temporal oxygen data to improve the quantification of in situ petroleum biodegradation rates. J. Environ. Manage. 117:42-49.

533 Dobson, R., M.H. Schroth, and J. Zeyer. 2007. Effect of water-table fluctuation on
534 dissolution and biodegradation of a multi-component, light nonaqueous-phase liquid.
535 J. Contam. Hydrol. 94:235-248.
536 Dutta, T., A. Carles-Brangari, D. Fernandez-Garcia, S. Rubola, J. Tirado-Conde, and X.
537 Sanchez-Vila. 2015. Vadose zone oxygen (O_2) dynamics during drying and wetting
538 cycles: An artificial recharge laboratory experiment. J. Hydrol. 527:151-159.
539 Farnsworth, C.E., and J.G. Hering. 2011. Inorganic geochemistry and redox dynamics in
540 bank filtration settings. Environ. Sci. Technol. 45(12):5079-5087.
541 Farnsworth, C.E., A. Voegelin, and J.G. Hering. 2012. Manganese oxidation induced by
542 water table fluctuations in a sand column. Environ. Sci. Technol. 46:277-284.
543 Gillefalk, M., G. Massmann, G. Nützmann, and S. Hilt. 2018. Potential impacts of
544 induced bank filtration on surface water quality: A conceptual framework for future
545 research. Water 10(9):1240.
546 Guo, Y.Z., Y.P. Zhao, T.T. Zhu, J.Q. Li, Y. Feng, H.Z. Zhao, and S.T. Liu. 2018. A
547 metabolomic view of how low nitrogen strength favors anammox biomass yield and
548 nitrogen removal capability. Water Res. 143:387-398.
549 Haberer, C.M., M. Rolle, O.A. Cirpka, and P. Grathwohl. 2012. Oxygen transfer in a
550 fluctuating capillary fringe. Vadose Zone J. 11(3):811-822.
551 Haberer, C.M., M. Rolle, O.A. Cirpka, and P. Grathwohl. 2014. Impact of heterogeneity
552 on oxygen transfer in a fluctuating capillary fringe. Ground Water 53(1):57-70.
553 Haberer, C.M., J.W. Roy, and J.E. Smith. 2015. Patterns of entrapped air dissolution in a
554 two-dimensional pilot-scale synthetic aquifer. Ground Water 53(2):271-281
555 Hou, X.K., T.L. Li, S.K. Vanapalli, and Y. Xi. 2019. Water percolation in a thick
556 unsaturated loess layer considering the ground-atmosphere interaction. Hydrol.
557 Process 33:794-802.
558 Huang, L.L., W.J. Hu, J. Tao, Y.Z. Liu, Z.Y. Kong, and L. Wu. 2019. Soil bacterial
559 community structure and extracellular enzyme activities under different land use
560 types in a long-term reclaimed wetland. J. Soils Sediments 19:2543-2557.
561 Jost, D, C.M. Haberer, P. Grathwohl, J. Winter, and C. Gallert. 2015. Oxygen transfer in
562 a fluctuating capillary fringe-Impact of microbial respiratory activity. Vadose Zone J.
563 14(5):1-14.
564 Kohfahl, C., G. Massmann, and A. Pekdeger. 2009. Sources of oxygen flux in
565 groundwater during induced bank filtration at a site in Berlin, Germany. J. Hydrol.
566 17(3):571-578.
567 Kolehmainen, R.E., J.H. Langwaldt, and J.A. Puhakka. 2007. Natural organic matter
568 (NOM) removal and structural changes in the bacterial community during artificial
569 groundwater recharge with humic lake water. Water Res. 41:2715-2725.
570 Kong, J., P. Xin, G.F. Hua, Z.Y. Luo, C.J. Shen, D. Chen, and L. Li. 2015. Effects of
571 vadose zone on groundwater table fluctuations in unconfined aquifers. J. Hydrol.
572 528:397-407.

573 Krause, S., A. Bronstert, and E. Zehe. 2007. Groundwater- surface water interactions in a
574 North German lowland floodplain - Implications for the river discharge dynamics
575 and riparian water balance. J. Hydrol. 347(3-4):404-417.
576 Li, D., M. Alidina, M. Ouf, J.O. Sharp, P. Saikaly, and J.E. Drewesa. 2013. Microbial
577 community evolution during simulated managed aquifer recharge in response to
578 different biodegradable dissolved organic carbon (BDOC) concentrations. Water
579 Res. 47(7): 2421-2430.
580 Lipson, D.A., D. Zona, T.K. Raab, F. Bozzolo, M. Mauritz, and W.C. Oeche. 2012.
581 Water-table height and microtopography control biogeochemical cycling in an
582 Arctic coastal tundra ecosystem. Biogeosciences 8(4):577-591.
583 Liu, L., S.Q. Wang, X.P. Guo, T.N. Zhao, and B.L. Zhang. 2018a. Succession and
584 diversity of microorganisms and their association with physicochemical properties
585 during green waste thermophilic composting. Waste Manage. (Oxford), 73:101-112.
586 Liu, S.J., B.D. Xi, Z.P. Qiu, X.S. He, H. Zhang, Q.L. Dang, X.Y. Zhao, and D. Li. 2019.
587 Succession and diversity of microbial communities in landfills with depths and ages
588 and its association with dissolved organic matter and heavy metals. Sci. Total
589 Environ. 651:909-916.
590 Liu, X.H., Y. Liu, S.Y. Lu, X.C. Guo, H.B. Lu, P. Qin, B. Bi, Z.F. Wan, B.D. Xi, T.T.
591 Zhang, and S.S. Liu. 2018b. Occurrence of typical antibiotics and source analysis
592 based on PCA-MLR model in the East Dongting Lake, China. Ecotox. Environ. Safe.
593 163:145-152.
594 Liu, Y.X., M. Luo, R.Z. Ye, J.F. Huang, L.L. Xiao, Q.K. Hu, A.J. Zhu, and C. Tong.
595 2019. Impacts of the rhizosphere effect and plant species on organic carbon
596 mineralization rates and pathways, and bacterial community composition in a tidal
597 marsh. FEMS Microbio. Ecol. 95(9):120.
598 Machler, L., S. Peter, M.S. Brennwald, and R. Kipfer. 2013. Excess air formation as a
599 mechanism for delivering oxygen to groundwater. Water Resour. Res.
600 49(10):6847-6856.
601 McLeod, H.C., J.W. Roy, and J.E. Smith. 2015. Patterns of entrapped air dissolution in a
602 two-dimensional pilot-scale synthetic aquifer. Ground Water 53 (2):271-281.
603 Meckenstock, R.U., M. Elsner, C. Griebler, T. Lueders, C. Stumpp, J. Aamand, S.N.
604 Agathos, H.J. Albrechtsen, L. Bastiaens, P.L. Bjerg, N. Boon, W. Dejonghe, W.E.
605 Huang, S.I. Schmidt, E. Smolders, S.R. Sørensen, D. Springael, and B.M. van
606 Breukelen. 2015. Biodegradation: updating the concepts of control for microbial
607 cleanup in contaminated aquifers. Environ. Sci. Technol. 49:7073-7081.
608 Miao, L.Z., C. Wang, J. Hou, P.F. Wang, Y.H. Ao, Y. Li, Y. Yao, B.W. Lv, Y.Y. Yang,
609 G.X. You, Y. Xu, and Q.H. Gu. 2017. Response of wastewater biofilm to CuO
610 nanoparticle exposure in terms of extracellular polymeric substances and microbial
611 community structure. Sci. Total Environ. 579:588-597.
612 Neale, C.N., J.B. Hughes, and C.H. Ward. 2000. Impacts of unsaturated zone properties
613 on oxygen transport and aquifer reaeration. Ground Water 38(5):784-794.

614 Ning, Z., M. Zhang, Z. He, P.P. Cai, C.J. Guo, and P. Wang. 2018. Spatial pattern of
615 bacterial community diversity formed in different groundwater field corresponding
616 to electron donors and acceptors distributions at a petroleum-contaminated site.
617 Water 10:842.
618 Niu, B.B., H.H. Wang, H.A. Loáiciga, S. Hong, and W. Shao. 2017. Temporal variations
619 of groundwater quality in the Western Jianghan Plain, China. Sci. Total Environ.
620 578:542-550.
621 Pett-Ridge, J., and M.K. Firestone. 2005. Redox fluctuation structures microbial
622 communities in a wet tropical soil. Appl. Environ. Microbiol. 71:6998-7007.
623 Rühle, F.A., F. von Netzer, T. Lueders, and C. Stumpp. 2015. Response of transport
624 parameters and sediment microbiota to water table fluctuations in laboratory
625 columns. Vadose Zone J. 14 (5):12. doi:10.2136/vzj2014.09.0116
626 Scheff, G., O. Salcher, and F. Lingens. 1984. Trichococcus-flocculiformis gen
627 nov-sp-nov- a new gram-positive filamentous bacterium isolated from
628 bulking-sludge. Appl. Microbiol. Biotechnol. 19 (2):114-119.
629 Schimel, J., T.C. Balser, and M. Wallenstein. 2007. Microbial stresses response
630 physiology and its implications for ecosystem function. Ecology 88:1368-1394.
631 Suenaga, T., S. Riya, M. Hosomi, and A. Terada. 2018. Biokinetic characterization and
632 activities of N_2O-reducing bacteria in response to various oxygen levels. Front.
633 Microbiol. 9:697.
634 Unno, T., J. Kima, Y. Kim, S.G. Nguyen, R.B. Guevarra, G.P. Kim, J.H. Lee, and M.J
635 Sadowsky. 2015. Influence of seawater intrusion on microbial communities in
636 groundwater. Sci. Total Environ. 532:337-343.
637 Van Driezum, I.H., A.H.S. Chik, S. Jakwerth, G. Lindner, A.H. Farnleitner, R. Sommer,
638 A.P. Blaschke, A.K.T. Kirschner. 2018. Spatiotemporal analysis of bacterial
639 biomass and activity to understand surface and groundwater interactions in a highly
640 dynamic riverbank filtration system. Sci. Total Environ. 627:450-461.
641 Voisin, J., B. Cournoyer, A .Vienney, and F. Mermillod-Blondin. 2018. Aquifer recharge
642 with stormwater runoff in urban areas: Influence of vadose zone thickness on
643 nutrient and bacterial transfers from the surface of infiltration basins to groundwater.
644 Sci. Total Environ. 637-638:1496-1507.
645 Vos, C., A. Don, E.U. Hobley, R. Prietz, A. Heidkamp, and A. Freibauer. 2019. Factors
646 controlling the variation in organic carbon stocks in agricultural soils of Germany.
647 Eur. J. Soil Sci. 70:550-564.
648 Wang, Q.F., M.C. Ma, X. Jiang, B.K. Zhou, D.W. Guan, F.M. Cao, S.F. Chen, and J. Li.
649 2019. Long-term N fertilization altered ^{13}C-labeled fungal community composition
650 but not diversity in wheat rhizosphere of Chinese black soil. Soil Biol. Biochem.
651 135:117-126.
652 Wang, X.D., X.J. Bi, L.J. Hem, and H. Ratnaweera. 2018. Microbial community
653 composition of a multi-stage moving bed biofilm reactor and its interaction with
654 kinetic model parameters estimation. J. Environ. Manag. 218:340-347.

655 Yang, Y.S., P.P. Li, X. Zhang, M.J. Li, Y. Lu, B. Xu, and T. Yu. 2017. Lab-based
656 investigation of enhanced BTEX attenuation driven by groundwater table fluctuation.
657 Chemosphere 169:678-684.
658 Yin, F.B., H.M. Dong, W.Q. Zhang, Z.P. Zhu, B. Shang, and Y. Wang. 2019. Removal of
659 combined antibiotic (florfenicol, tylosin and tilmicosin) during anaerobic digestion
660 and their relative effect. Renew. Energ. 139:895-903.
661 Zheng, L., M.L. Ren, E. Xie, A.Z. Ding, Y. Liu, S.Q. Deng, and D.Y. Zhang. 2019. Roles
662 of phosphorus sources in microbial community assembly for the removal of organic
663 matters and ammonia in activated sludge. Front. Microbiol. 10:1023.
664 Zhou, A.X., Y.L. Zhang, T.Z. Dong, X.Y. Lin, and X.S. Su. 2015. Response of the
665 microbial community to seasonal groundwater level fluctuations in petroleum
666 hydrocarbon-contaminated groundwater. Environ. Sci. Pollut. Res.
667 22(13):10094-10106.
668 Zhou, Z.D., T.T. Yan, Q. Zhu, X.L. Bu, B. Chen, J.H. Xue, and Y.B. Wu. 2019. Bacterial
669 community structure shifts induced by biochar amendment to karst calcareous soil in
670 southwestern areas of China. J. Soils Sediments 19:356-365.

672 **Figure captions**

673 **Fig. 1.** Schematic of the experimental system. QSC represents the quasi static column,
674 NFC represents the natural fluctuation column and RIC represents the rainfall infiltration
675 column.

676 **Fig. 2.** Spatio-temporal distribution of water saturation within the columns. Monitoring
677 points are in the vadose (a) and oscillated zones (b) of quasi static column (QSC), natural
678 fluctuation column (NFC) and rainfall infiltration column (RIC). Water saturation was
679 monitored every half hour.

680 **Fig. 3.** Spatio-temporal distribution of the oxygen level within the columns. Monitoring
681 points are in the vadose (a), oscillated (b) and saturated zones (c) of quasi static column
682 (QSC), natural fluctuation column (NFC) and rainfall infiltration column (RIC). Oxygen
683 level was monitored every half hour.

684 **Fig. 4.** Variation in soil TOC removal at the end of the experiments as a function of depth,
685 the error bars represent the standard deviation of the mean values. * indicates a
686 significant difference at $P < 0.05$.

687 **Fig. 5.** Relative abundance of major bacteria at the phylum (a) and heat map of top 20
688 most abundant classes (b). The relative abundance is presented as the percentage of the
689 total effective bacterial sequences in each sample.

690 **Fig. 6.** Redundancy analysis for the relationship between samples, bacterial community
691 diversity, structure, water saturation, oxygen level and TOC removal. Circles represent
692 the QSC, triangles represent the NFC and squares represent the RIC; red arrows represent

693 water saturation, oxygen level and TOC removal; cyan arrows represent bacterial
694 community diversity indices; blue arrows represent dominant bacterial species.
695

697 **Table 1.** Bacterial community diversity indices.

	Vadose zone			Oscillated zone			Saturated zone		
	QSC_V	NFC_V	RIC_V	QSC_O	NFC_O	RIC_O	QSC_S	NFC_S	RIC_S
Good's coverage	0.9546	0.9537	0.9587	0.9503	0.9495	0.9500	0.9539	0.9549	0.9443
Chao 1	1978	1999	1854	2188	2207	2173	1954	1917	2316
Shannon	9.17	9.13	9.09	9.43	9.43	9.43	8.87	8.73	9.20

698 QSC: the quasi static column; NFC: the natural fluctuation column; RIC: the rainfall infiltration
699 column. V: the vadose zone; O: the oscillated zone; S: the saturated zone.
700

Table 2. Pearson correlation between geochemical parameters and bacterial communities.

	Water saturation	Oxygen level	TOC removal rate
Betaproteobacteria	-0.026	-0.064	0.423
Alphaproteobacteria	-0.598	0.676*	-0.207
Deltaproteobacteria	0.618	-0.629	0.827*
Sphingobacteriia	0.857**	-0.906**	0.445
Gammaproteobacteria	-0.526	0.591	-0.096
Bacilli	0.650	-0.682*	0.437
Clostridia	0.566	-0.470	0.426
Gemmatimonadetes	-0.691*	0.751*	-0.786*
Cytophagia	0.732*	-0.580	0.476
Actinobacteria	-0.806**	0.717*	-0.641

* indicates correlation significant at $P < 0.05$

** indicates correlation significant at $P < 0.01$.

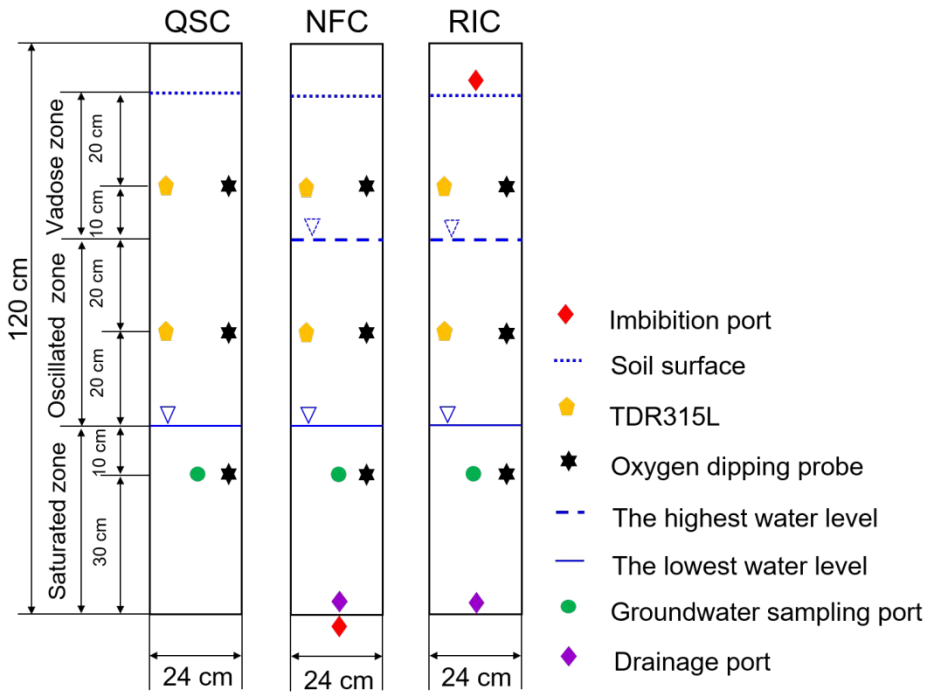

Fig. 1. Schematic of the experimental system. QSC represents the quasi static column, NFC represents the natural fluctuation column and RIC represents the rainfall infiltration column.

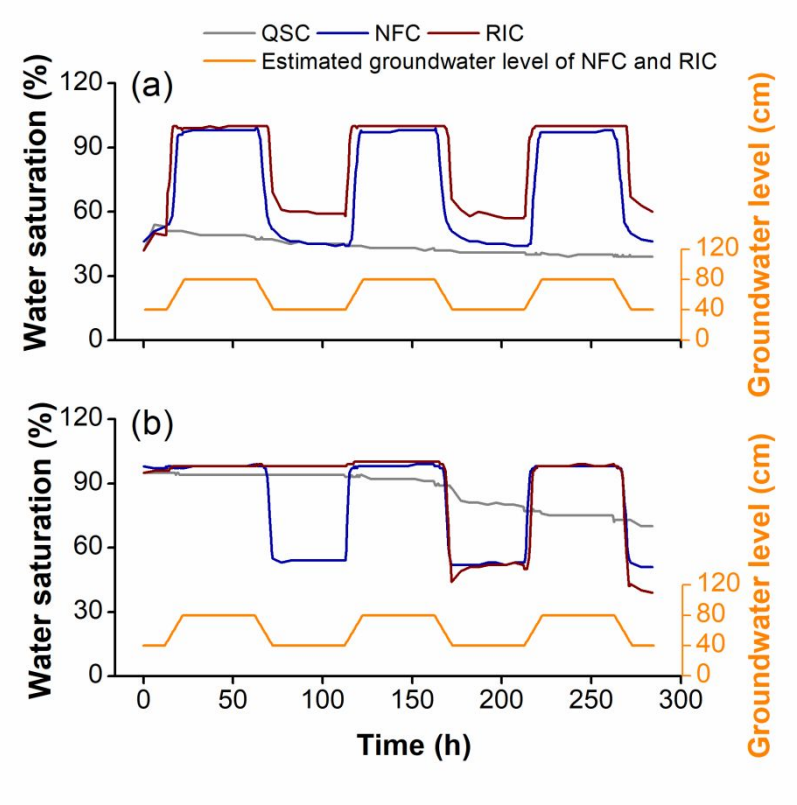

Fig. 2. Spatio-temporal distribution of water saturation within the columns. Monitoring points are in the vadose (a) and oscillated zones (b) of quasi static column (QSC), natural fluctuation column (NFC) and rainfall infiltration column (RIC). Water saturation was monitored every half hour.

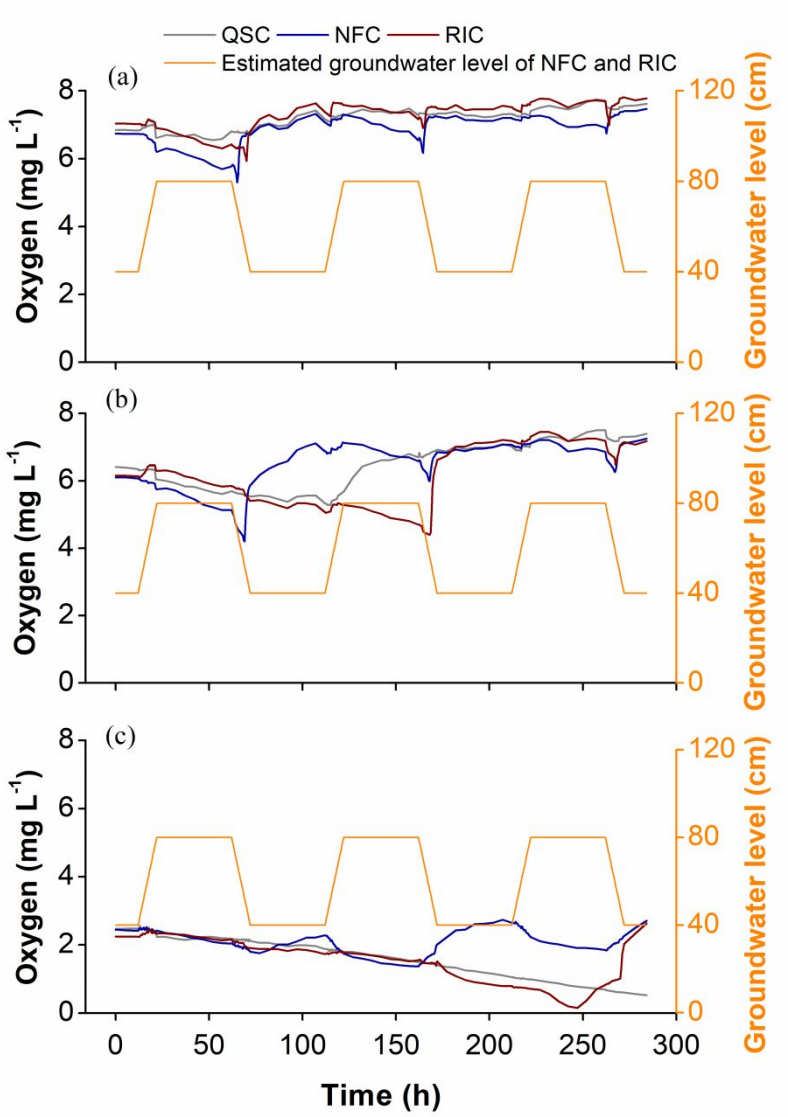

Fig. 3. Spatio-temporal distribution of the oxygen level within the columns. Monitoring points are in the vadose (a), oscillated (b) and saturated zones (c) of quasi static column (QSC), natural fluctuation column (NFC) and rainfall infiltration column (RIC). Oxygen level was monitored every half hour.

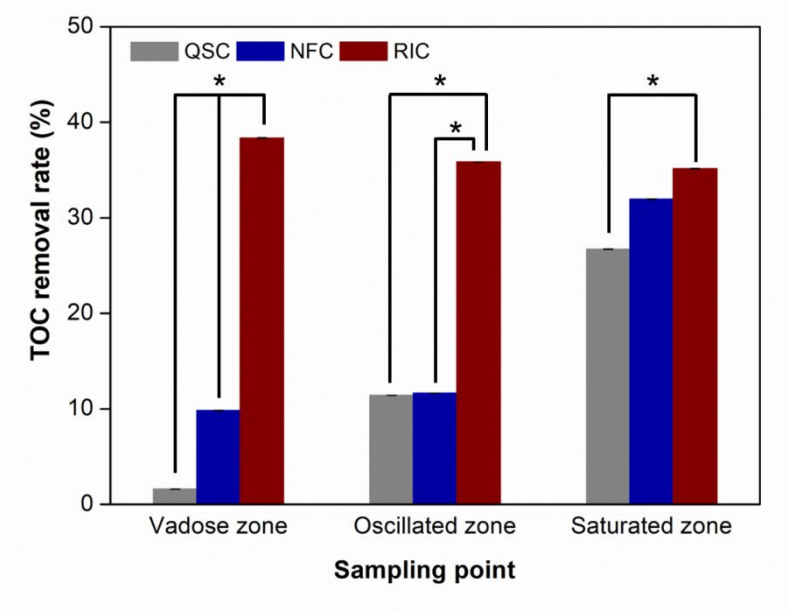

Fig. 4. Variation in soil TOC removal at the end of the experiments as a function of depth, the error bars represent the standard deviation of the mean values. * indicates a significant difference at $P < 0.05$.

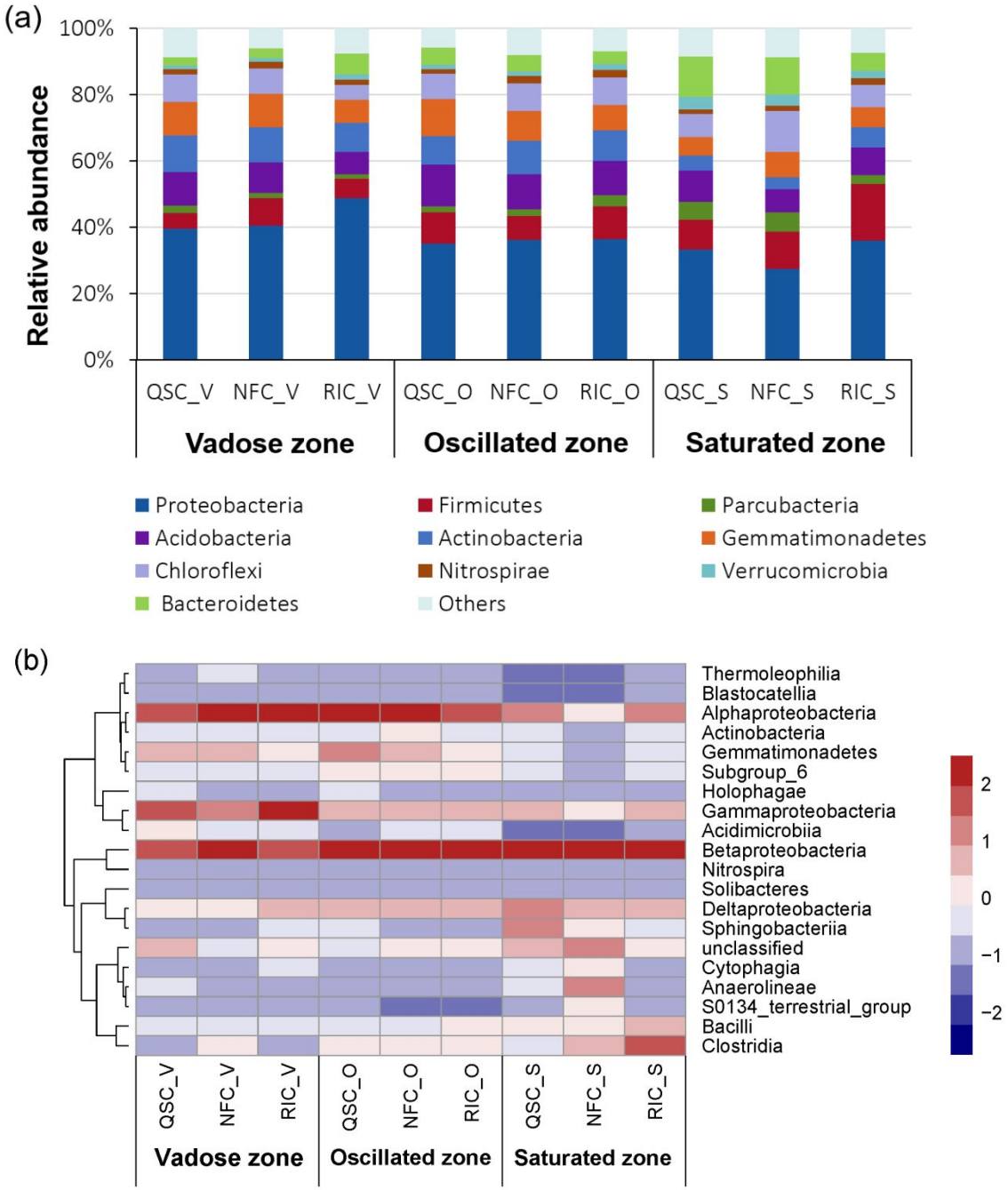

Fig. 5. Relative abundance of major bacteria at the phylum (a) and heat map of top 20 most abundant classes (b). The relative abundance is presented as the percentage of the total effective bacterial sequences in each sample.

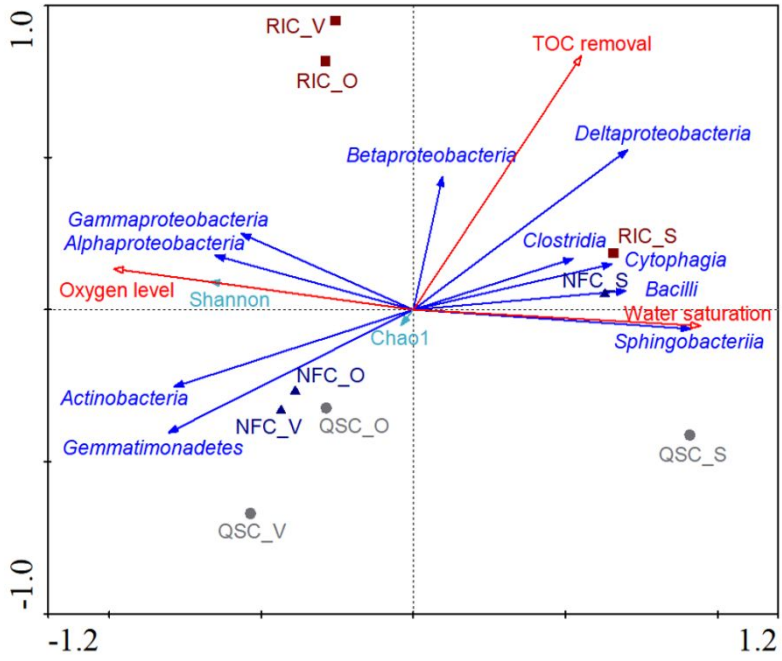

Fig. 6. Redundancy analysis for the relationship between samples, bacterial community diversity, structure, water saturation, oxygen level and TOC removal. Circles represent the QSC, triangles represent the NFC and squares represent the RIC; red arrows represent water saturation, oxygen level and TOC removal; cyan arrows represent bacterial community diversity indices; blue arrows represent dominant bacterial species.

Supplementary material

For

Response of soil bacterial community composition and its associated geochemical parameters to rapid short-term cyclic groundwater-level oscillations: soil column experiments

Xuefeng Xia[a,c,d], Lirong Cheng[a,c,d], Yi Zhu[a,c,d], Yueqiao Liu[a,c,d], Kai Wang[a,c,d], Aizhong Ding[a,c,d,*], Zuansi Cai[b], Huansheng Shi[e], and Lili Zuo[e]

[a] College of Water Sciences, Beijing Normal University, Beijing 100875, China

[b] School of Engineering and the Built Environment, Edinburgh Napier University, Edinburgh EH10 5DT, UK

[c] Engineering Research Center of Groundwater Pollution Control and Remediation of Ministry of Education, Beijing Normal University, Beijing 100875, China

[d] Beijing Key Laboratory of Urban Hydrological Cycle and Sponge City Technology, Beijing Normal University, Beijing 100875, China

[e] China Railway Fifth Survey and Design Institute Group Co., Ltd., Beijing 102600, China

*Corresponding author

Email: ading@bnu.edu.cn

Table S 1. Physical and chemical properties of soil. TOC represents total organic carbon.

Parameter		Value
Water saturation (%)		0.10
Bulk density (g cm^{-3})		1.32
TOC (g kg^{-1})		1.46
Size distribution (%)	< 0.02 mm	4.36
	0.02-0.1 mm	11.14
	0.1-0.25 mm	13.84
	0.25-1 mm	64.81
	> 1 mm	5.85

Table S 2. Physical and chemical properties of groundwater and rainfall water. DO represents dissolved oxygen; DOC represents dissolved organic carbon.

Parameter		Value
Groundwater	DO (mg L^{-1})	1 ± 0.2
	DOC (mg L^{-1})	3.392
	NO_3^- (mg L^{-1})	3.705
	SO_4^{2-} (mg L^{-1})	30.440
Rainfall water	DO (mg L^{-1})	8 ± 0.5
	DOC (mg L^{-1})	3.392
	NO_3^- (mg L^{-1})	3.705
	SO_4^{2-} (mg L^{-1})	30.440
Volume of imbibed or drained water (mL)		6330

Water saturation and oxygen monitoring

Two 21.5 cm long three-pronged stainless-steel TDR315L probes were embedded vertically at depths of about 80 - 100 cm and 50 - 70 cm above the bottom during packing, combined with a data collector CR300 (Campbell, America), we monitored volumetric water content in the vadose zone and oscillated zone, respectively. Water saturation was calculated by the ratio of measured volumetric water content with soil porosity.

Three 10 cm long oxygen dipping probes (PreSens, Germany) were dipped at depths of 90 cm, 60 cm and 30 cm above the bottom, combined with an OXY-10 trace SMA monitoring technique (PreSens, Germany), we monitored oxygen level (we detected the measurement signals inside of the column that correspond to values of oxygen partial pressure which were then converted into the respective values of volumetric aqueous concentration) in vadose zone, oscillated zone and saturated zone, respectively.

Analytical methods of groundwater quality variations

Groundwater samples were collected from the continuously saturated zone (30 cm above the bottom) of QSC, NFC and RIC. Each groundwater sample was analyzed less than 24 h after being collected. DOC was measured using a Vario TOC (Elementar, Germany). UV-Visible measurements were performed using a UV-2600 spectrophotometer (Shimadzu, Japan) at the wavelength scanning range of 200-300 nm, with Milli-Q water used as control group to obtain the absorption spectrum of the samples. The ultraviolet absorbance $SUVA_{254}$ characterizes the unsaturated degree of dissolved organic matter (DOM) and represents the relative content of aromatic ring or unsaturated double bond compounds in DOM (Guo et al., 2011). The E_{253}/E_{203} was the absorbance ratio ranged between 253 and 203 nm that is related to oxygen-containing functional groups, represents the stability of DOM with aromatic structure, and a larger value corresponds to greater stability and a reduced likelihood of degradation (Liu et al., 2019).

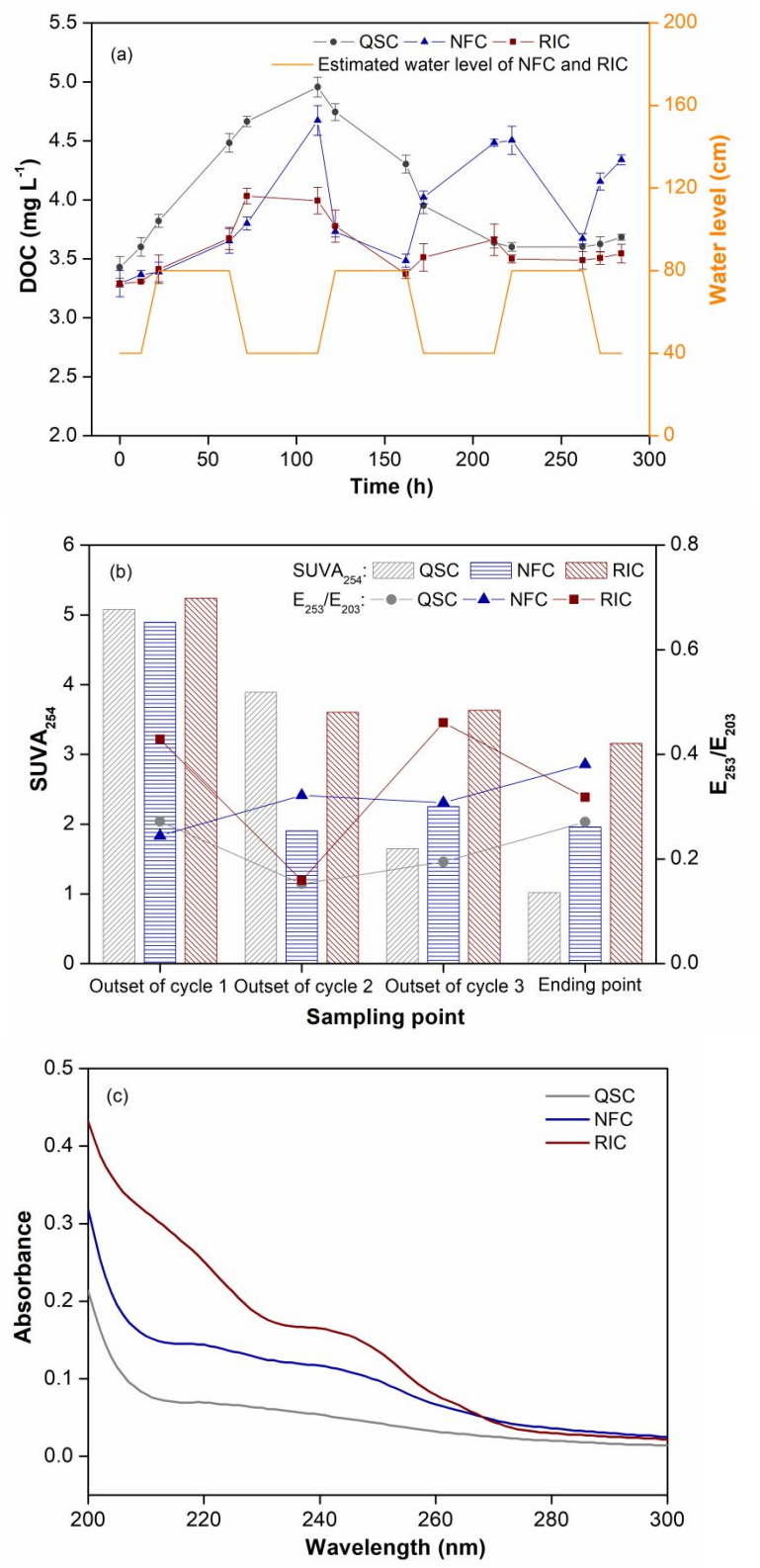

Fig. S. 1. Groundwater DOC time series over the entire period of groundwater-level oscillations (a), the error bars represent the standard deviation of the mean values. Changes of characterized absorbance $SUVA_{254}$ and $E_{253/203}$ during groundwater-level

oscillations (b); UV spectrum at the end of the experiment (c). Sampling points were located 30 cm above the bottom in quasi static column (QSC), natural fluctuation column (NFC) and rainfall infiltration column (RIC).

Soil sample collection

Soil sampling were performed by a 120 cm (diameter: 1.25 cm) direct push manual sampler (AMS, America). The sampler is a dual-tube sampling system, which can be hammered into the soil using a rubber mallet to collect undisturbed and depth-specific samples by replacing the inner tubes and extracted by hand. Soil samples were collected from depths of 89 - 91 cm, 59 - 61 cm and 29 - 31 cm above the bottom of the QSC, NFC and RIC. These three depths represent vadose, oscillated and saturated zones, respectively.

Polymerase chain reaction (PCR)

For each sample, 10-digit barcode sequence was added to the 5' end of the forward and reverse primers. The reaction mixture consisted of DNA template (30 ng), 1 μL of each primer (5 μM), 3 μL of BSA (2 ng/μL), 12.5 μL of 2×Taq PCR MasterMix and 7.5 μL of double distilled H_2O. PCR was performed under the following conditions: 5 min at 94 °C followed by 25 cycles of 30 s at 94 °C, 30 s at 50 °C, and 1 min at 72 °C and then 7 min at 72 °C.

High-quality sequences extraction

Raw reads shorter than 110 nucleotides, truncated reads that were shorter than 50 bp, two nucleotide mismatch in primer matching and reads containing ambiguous characters, or overlap shorter than 10 bp were removed (Yin et al., 2019).

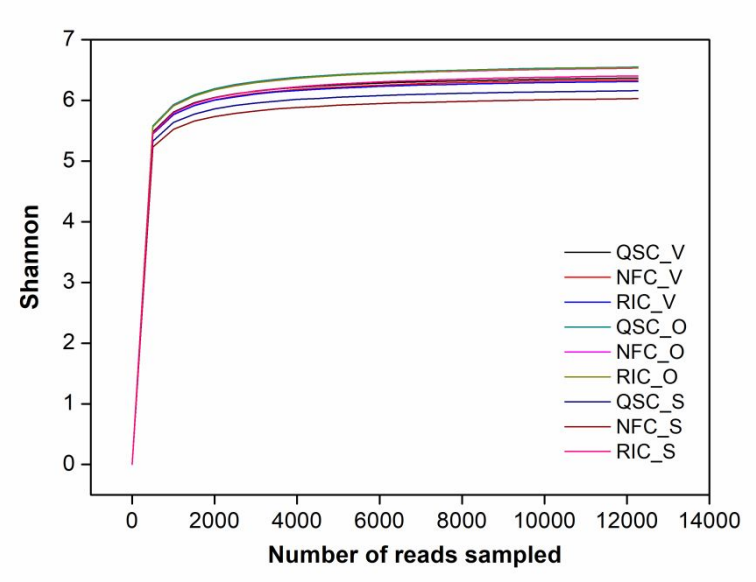

Fig. S. 2. Shannon-Wiener curve of all the soil samples. QSC represents the quasi static column, NFC represents the natural fluctuation column and RIC represents the rainfall infiltration column. V represents the vadose zone; O represents the oscillated zone; S represents the saturated zone.

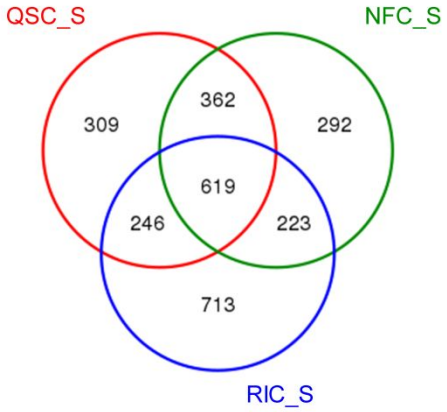

Fig. S. 3. Venn diagram of bacterial community diversity in the saturated zone (S) of quasi static column (QSC), natural fluctuation column (NFC) and rainfall infiltration column (RIC). S represents the saturated zone.

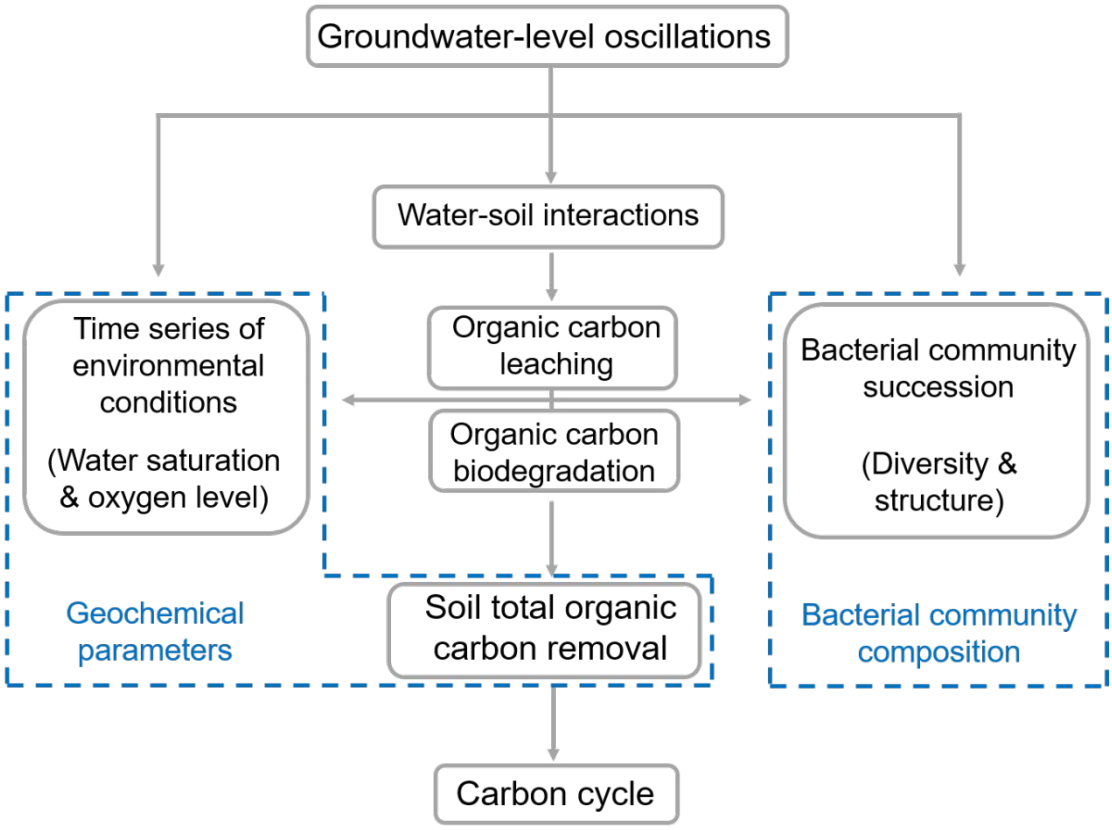

Fig. S. 4. Proposed flow diagram of carbon cycle during groundwater-level oscillations.

References

Guo, X.J., B.D. Xi, H.B. Yu, W.C. Ma and X.S. He. 2011. The structure and origin of dissolved organic matter studied by UV-vis spectroscopy and fluorescence spectroscopy in lake in arid and semi-arid region. Water Sci. Technol. 63(5):1010-1017.

Liu, S.J., B.D. Xi, Z.P. Qiu, X.S. He, H. Zhang, Q.L. Dang, X.Y. Zhao, and D. Li. 2019. Succession and diversity of microbial communities in landfills with depths and ages and its association with dissolved organic matter and heavy metals. Sci. Total Environ. 651:909-916.

Yin, F.B., H.M. Dong, W.Q. Zhang, Z.P. Zhu, B. Shang, and Y. Wang. 2019. Removal of combined antibiotic (florfenicol, tylosin and tilmicosin) during anaerobic digestion and their relative effect. Renew. Energ. 139:895-903.